Spectroscopy 20 (2006) 275–283
IOS Press

FT-IR spectra and vibrational spectroscopy of Andrographolide

P.K. Singh [a], Tanveer Hasan [a], Onkar Prasad [a], Leena Sinha [b], Kanwal Raj [c] and Neeraj Misra [a,*]

[a] *Department of Physics, Lucknow University, 226007, India*
[b] *Department of Physics, Mahila PG College, Aminabad, Lucknow, India*
[c] *Medicinal and Process Chemistry Division, Central Drug Research Institute, Lucknow, 226001, India*

Abstract. A complete normal coordinate analysis was performed for andrographolide in terms of the calculation by using Wilson's G-F matrix method and Urey Bradley force field. Normal coordinate analysis has been carried out to understand the dynamical behaviour of the bioactive labdane diterpenoid of the medicinally useful terrestrial plant Andrographis paniculata. The structural elucidation of a novel, biologically active natural product followed by its total synthesis lays the groundwork for investigations into its biological mechanism of action including putative cellular receptor isolation.

Keywords: FT-IR spectra, diterpene, normal coordinate analysis

1. Introduction

Natural products hold great potential as probes of the cellular processes in which they interfere. Structural and conformational studies lead to hypothesis concerning target ligand interactions while synthesis is a means to test these hypotheses by eventual total synthesis of derivatives. Andrographis has long been used in traditional Indian and Chinese herbal medicine. The most common reported uses were for digestive problems (as is the case with most non toxic bitter herbs such as andrographis) snake bite, and infections ranging from malaria to dysentery [1,2]. Interestingly some of these uses have been validated by modern scientific research. The major constituents in andrographis are diterpene lactones known as andrographolide. These bitter constituent are believed to have immune-stimulating, anti inflammatory, fertility decreasing, liver protective and bile secretion-stimulating actions [3]. Though some older studies suggested andrographis was antibacterial, modern research has been unable to confirm this finding [4]. Although, a number of studies on the structure and stability of andrographolide have been carried out [5–9]. To the best of our knowledge no study on the normal coordinate analysis on andrographolide has been reported so far in the literature.

As a part of our ongoing research work [10–17] on vibrational analysis, phonon dispersion, phase transition in a variety of macromolecules, here in the present communication we report the dynamical study carried out on the diterpene Andrographolide. The purpose of this study assumes importance because of the further work on andrographolide (i.e., oxidation studies on Andrographolide) [18], in

*Corresponding author: Neeraj Misra, Department of Physics, Lucknow University, 226007, India. E-mail: misraneeraj@gmail.com

which presumably some modification by chemical reaction such as oxidation/reduction on poly functional bioactive natural product will generate new reactive site in the molecule, which can be exploited for elaborating and appending pharmacophores to generate patentable compounds of biological interest.

2. Theory

The well known Wilson's G-F Matrix method [19–21] with Urey Bradley [22] force field has been used to evaluate the normal modes.

These are given by the eigen values λ of the secular equation.

$$\text{GFL} = \lambda L \quad \text{as} \quad \lambda = 4\pi^2 c^2 v^2.$$

The potential is represented as

$$V = \sum_{jk} K'_{jk} r_{jk}(\Delta r_{jk}) + \frac{1}{2} K_{jk}(\Delta r_{jk})^2 + \sum_{ijk} H'_{ijk} r_{ij} r_{jk}(\Delta\phi_{ijk}) + \frac{1}{2} H_{ijk} r_{ij} r_{jk}(\Delta\phi_{ijk})^2 + \sum_{ijk} F'_{ik} q_{ik}(\Delta q_{ik}) + \frac{1}{2} F_{ik}(\Delta q_{ik})^2 + \sum_{i} K_j^w(\Delta w_j)^2 + \sum_{j} K_j^t(\Delta t_j)^2,$$

where $\Delta r_{jk}, \Delta\phi_{ijk}, \Delta w_j$ and Δt_j are the internal coordinate changes corresponding to bond stretch, angle bend, out of plane deformation and torsion respectively.

The potential energy distribution in the jth internal coordinate for the ith normal mode is given by

$$(\text{PED}) = \frac{L^*_{ji} L_{ji} F_{ji}}{\lambda_i}.$$

3. Experimental

The FTIR spectra of andrographolide have been recorded in CsI on a Perkin Elmer 1800 spectrophotometer. Spectroscopic preparation of sample were carried out under an atmosphere of prepurified nitrogen.Andrographolide was isolated from fresh plant material of Andrographis paniculata to the procedure reported in literature [23]. The compound was identified by comparison with its IR, MS, NMR data with that of reported in literature [22,24].

4. Results and Discussion

4.1. Structure

The crystal structure of Andrographolide has been reported by several workers [24,25] but the present structure is more accurately determined. The six membered rings are in chair conformation. The furan ring is slightly puckered. The molecule crystallizes in space group $P2_1$ with the monoclinic unit cell. Basak et al. [26,27] have shown that andrographolide could be considered as an important precursor structure that might require further structural modification for enhancement of its enzyme inactivation

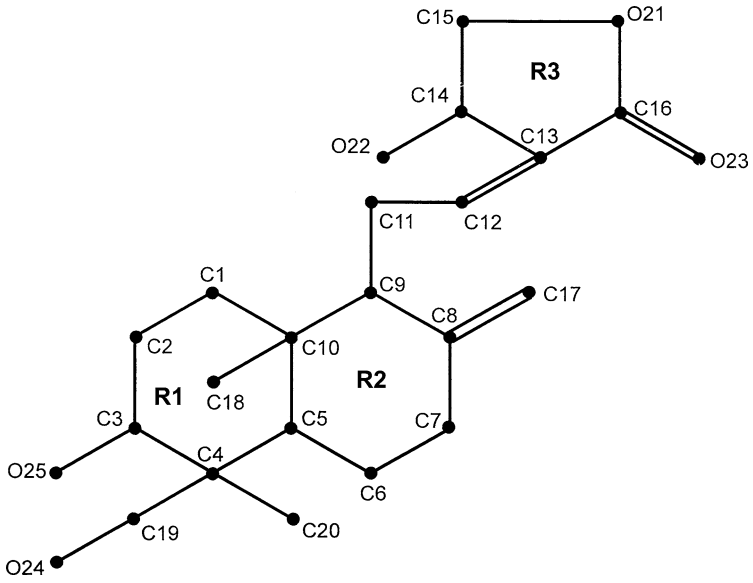

Fig. 1. Model molecular structure of Andrographolide.

property. The modification of hydroxy groups in Andrographis paniculata could lead to a better understanding of its inhibitory action. The actual mechanism by which these diterpenes exert their inhibitory action against convertases is not currently understood but these molecules do contain a highly reactive five membered lactone ring. In andrographolide, the entire structure is essential for biological action and presumably the vibrational modes involving the sites with substantial potential energy contribution play a decisive role in the receptor binding. This justifies the need for an in depth study of the conformation and dynamics of andrographolide.

4.2. Vibrational Investigations

Normal coordinate calculations were performed using the program developed by Shimanouchi [28] following the G-F matrix method according to Wilson et al. This method describes the motion in terms of the internal coordinates, which are changes in bond lengths, bond angles and those out of plane bending and dihedral angles. The force constants in terms of these coordinates can be easily visualized and have a physical meaning. We have used a Urey Bradley force field in our calculations. It incorporates intra unit interactions and interactions due to the neighboring units, in addition to the bonded interactions. It also includes the interactions between non-bonded atoms. Force constants were initially taken from the literature [19] and later modified to give the "best fit" with the observed FT-IR spectra.

The andrographolide has 55 atoms, however to reduce the problem to manageable dimensions CH, CH_2, CH_3 have been treated as mass points with a mass of 13, 14 and 15 respectively. This does not in any way disturb the accuracy of the results reported here. This is because the frequencies belonging to these can be well designated as group frequencies and many of them being in the higher range do not mix with other modes. With this approximation the andrographolide problem reduces to 25 atom problem with 69 normal modes of vibrations. The structural data used for Andrographolide is reported by Spek et al. [29]. The model molecular structure of andrographolide used in normal coordinate analysis is given in Fig. 1. The internal coordinates and force constants for Andrographolide are given in Table 1. The final

Table 1
Internal co-ordinates and urey bradley force constants (md/A^0)

Internal coordinate	Force constant	Internal coordinate	Force constant
1. ν(C1–C2)	3.531	47. ϕ(C8–C9–C10)	1.850 (1.080)
2. ν(C1–C10)	3.531	48. ϕ(C8–C9–C11)	0.480 (0.250)
3. ν(C2–C3)	3.531	49. ϕ(C10–C9–C11)	0.480 (0.250)
4. ν(C3–C4)	3.531	50. ϕ(C1–C10–C5)	1.520 (0.980)
5. ν(C3–O25)	4.900	51. ϕ(C1–C10–C9)	0.480 (0.250)
6. ν(C4–C5)	3.531	52. ϕ(C1–C10–C18)	0.480 (0.250)
7. ν(C4–C19)	5.830	53. ϕ(C5–C10–C9)	1.850 (1.080)
8. ν(C4–C20)	4.400	54. ϕ(C5–C10–C18)	0.480 (0.250)
9. ν(C5–C6)	3.290	55. ϕ(C9–C10–C18)	0.480 (0.250)
10. ν(C5–C10)	3.800	56. ϕ(C9–C11–C12)	0.680 (0.580)
11. ν(C6–C7)	3.290	57. ϕ(C11–C12=C13)	0.950 (0.750)
12. ν(C7–C8)	3.290	58. ϕ(C12=C13–C14)	0.650 (0.450)
13. ν(C8–C9)	3.290	59. ϕ(C12=C3–C16)	0.650 (0.450)
14. ν(C8=C17)	7.653	60. ϕ(C14–C13–C16)	0.651 (0.550)
15. ν(C9–C10)	3.290	61. ϕ(C13–C14–C15)	0.651 (0.550)
16. ν(C9–C11)	4.250	62. ϕ(C13–C14–O22)	1.010 (0.780)
17. ν(C10–C18)	4.400	63. ϕ(C15–C14–O22)	1.010 (0.780)
18. ν(C11–C12)	3.580	64. ϕ(C14–C15–O21)	0.550 (0.450)
19. ν(C12=C13)	5.630	65. ϕ(C13–C16–O21)	0.550 (0.450)
20. ν(C13–C14)	4.280	66. ϕ(C13–C16=O23)	1.250 (0.952)
21. ν(C13–C16)	4.280	67. ϕ(C21–C16=23)	1.550 (1.050)
22. ν(C14–C15)	4.280	68. ϕ(C4–C19–O24)	0.550 (0.350)
23. ν(C14–O22)	4.000	69. ϕ(C15–O21–C16)	0.412 (0.350)
24. ν(C15–O21)	6.060	70. ω(O22–C14)	0.500
25. ν(C16–O21)	4.755	71. ω(O23=C16)	0.380
26. ν(C16=O23)	9.239	72. ω(O25–C3)	0.500
27. ν(C19–O24)	6.580	73. ω(C17=C8)	0.500
28. ϕ(C2–C1–C10)	1.520 (0.980)	74. ω(C18–C10)	0.456
29. ϕ(C1–C2–C3)	1.520 (0.980)	75. ω(C20–C4)	0.456
30. ϕ(C2–C3–C4)	1.520 (0.980)	76. τ(C1–C2)	0.182
31. ϕ(C2–C3–O25)	0.760 (0.350)	77. τ(C1–C10)	0.182
32. ϕ(C4–C3–O25)	0.760 (0.350)	78. τ(C2–C3)	0.182
33. ϕ(C3–C4–C5)	1.520 (0.980)	79. τ(C3–C4)	0.182
34. ϕ(C3–C4–C19)	0.480 (0.250)	80. τ(C4–C5)	0.182
35. ϕ(C3–C4–C20)	0.480 (0.250)	81. τ(C4–C19)	0.182
36. ϕ(C5–C4–C19)	0.480 (0.250)	82. τ(C5–C6)	0.136
37. ϕ(C5–C4–C20)	0.480 (0.250)	83. τ(C5–C10)	0.182
38. ϕ(C19–C4–C20)	0.462 (0.350)	84. τ(C6–C7)	0.136
39. ϕ(C4–C5–C6)	0.480 (0.250)	85. τ(C7–C8)	0.136
40. ϕ(C4–C5–C10)	1.520 (0.980)	86. τ(C8–C9)	0.136
41. ϕ(C6–C5–C10)	1.850 (1.080)	87. τ(C9–C10)	0.136
42. ϕ(C5–C6–C7)	1.850 (1.080)	88. τ(C9–C11)	0.186
43. ϕ(C6–C7–C8)	1.850 (1.080)	89. τ(C11–C12)	0.185
44. ϕ(C7–C8–C9)	1.850 (1.080)	90. τ(C12=C13)	0.185
45. ϕ(C7–C8=C17)	0.750 (0.750)	91. τ(C13–C14)	0.181
46. ϕ(C9–C8=C17)	0.750 (0.750)	92. τ(C13–C16)	0.181
		93. τ(C14–C15)	0.181
		94. τ(C15–C21)	0.180
		95. τ(C16–O21)	0.060

Note:
ν(X–Y) represents the stretching between the atoms X and Y etc.
ϕ(X–Y–Z) represents the in plane bending between the atoms X, Y and Z.
ω(X–Y) represents the out of plane bending (wagging) between the atoms X and Y.
τ(X–Y) represents the torsion of the atoms X and Y.
The number in parenthesis represents the non-bonded value of the atoms X, Y and Z.

Table 2
Optimized force constant values for corresponding modes

S. No.	Modes	Force constant value
1	ν(C–C)R1	3.5310
2	ν(C–C)R2	3.2900
3	ν(C–C)R3	4.2800
4	ν(C–C)COM R1&R2	3.8000
5	ν(C–C)adj–R1	4.4000
6	ν(C=C)adj–R2	7.6530
7	ν(C–C)adj–R2	4.2500
8	ν(C=C)adj–R3	5.6380
9	ν(C–O)adj–R1	4.9000
10	ν(C=O)adj–R3	9.2390
11	ν(C–O)R3	6.0600
12	ν(C–O)link–R1	6.5800
13	ν(C–O)adj–R3	4.0000
14	ν(C–C)BB	3.5800
15	ν(C–C)adj–R1–O	5.8300
16	ν(C–O)R3–adj–O	4.7550
17	ϕ(C–C–C)R1	1.5200
18	ϕ(C–C–C)R2	1.8500
19	ϕ(C–C–C)R3	0.6510
20	ϕ(C–C–C)adj–R1&R2	0.4800
21	ϕ(C–C–C)BB	0.6800
22	ϕ(C–C=C)adj–R2	0.7500
23	ϕ(C–C–O)adj–R3	1.0100
24	ϕ(C–C–O)R3	0.5500
25	ϕ(O–C=O)adj–R3	1.5500
26	ϕ(C–C–O)link–R1	0.5500
27	ϕ(C–O–C)R3	0.4120
28	ϕ(C=C–C)adj–R3	0.6500
29	ϕ(C–C–C)adj–R1	0.4620
30	ϕ(C–C=O)adj–R3	1.2500
31	ϕ(C–C=C)BB	0.9500
32	ω(O–C)R1&R3	0.5000
33	ω(O=C)R3	0.3800
34	ω(C=C)R2	0.5000
35	ω(C–C)R1	0.4560
36	τ(C–C)R1	0.1820
37	τ(C–C)adj–R1–O	0.1820
38	τ(C–C)R2	0.1356
39	τ(C–C)common R1&R2	0.1820
40	τ(C–C)adj–R2	0.1856
41	τ(C–C)BB	0.1850
42	τ(C=C)adj–R3	0.1850
43	τ(C–C)R3	0.1810
44	τ(C–O)R3	0.1800
45	τ(C–O)R3–adj–O	0.0600

Note: Abbreviations used in the table have following meanings: R – Ring; Adj – Adjacent to; BB – Back Bone.

optimized force constant values for the corresponding modes are given in Table 2. The frequencies along with the potential energy distribution are given in Table 3. The FT-IR spectra of Andrographolide is given in Fig. 2. The observed frequencies agree with the calculated ones within 5 cm^{-1}. In the assignment of the normal modes only the dominant potential energy distributions are given. Identification with

Table 3
Calculated and observed vibrational modes of andrographolide

Calculated freq. cm^{-1}	Observed freq. cm^{-1}	Assignment (% Potential energy distribution)
1728	1728	ν(C=O)adj–R3 [77] + ν(C–C)R3 [18] + ν(C–O)R3adj-O [6] + ϕ(C–C-O) R3 [6]
1675	1675	ν(C=C)adj–R2 [67] + ϕ(C–C–C) R2 [26] + ν(C–C)R2 [12]
1596	1595	ν(C=C)adj–R3 [47] + ν(C–C)R3 [34] + ϕ(C–C=O)adj–R3 [11] + ν(C–O)R3adj-O [9] + ϕ(C–C–C) R3 [8] + ϕ(O–C=O)adj–R3 [6]
1455	1459	ν(C–C)com R1&R2 [44] + ϕ(C–C–C)R2 [16] + ϕ(C–C–C)R1 [15] ν(C–C)R2 [13] + ν(C–C)adj–R1 [10] + ν(C–C)adj–R2 [10] + ϕ(C–C–C)adj–R1&R2 [7]
1416	1420	ν(C–C)adj–R1–O [33] + ν(C–C)adj–R1 [19] + ϕ(C–C–C)R1 [10] + ν(C–C)–R1 [9] + ϕ(C–C–C)R2 [8] + ϕ(C–C–C)adj–R1&R2 [6] + ν(C–O)link–R1 [6]
1367	1367	ν(C–C)R1 [22] + ν(C–O)adj–R1 [22] + ν(C–C)R2 [16] + ϕ(C–C–C)R1 [15] ν(C–C)adj–R2 [11] + ν(C–C)adj–R1 [7] + ϕ(C–C–C)R2 [7]
1299	1297	ν(C–O)R3 [25] + ν(C–C)R3 [23] + ϕ(O–C=O)adj–R3 [11] + ϕ(C=C–C)adj–R3 [10] + ν(C=C)adj–R3 [8] + ν(C–C)BB [8]
1262	1266	ν(C–O)R3 [46] + ν(C–C)R3 [20] + ν(C–O)R3 adj-O [10] + ν(C=C)adj–R3 [9] + ν(C–C)BB [8]
1222	1220	ν(C–O)link–R1 [31] + ν(C–C)R2 [30] + ϕ(C–C–C)R2 [15] + ν(C–C)adj–R1 [11]
1157	1158	ν(C–C)R3 [60] + ν(C–O)R3 [16] + ν(C–O)adj–R3 [13] + ϕ(C–C-O)adj–R3 [9]
1085	1079	ν(C–O)adj–R3 [51] + ϕ(C–C-O)adj–R3 [14] + ν(C–C)R1 [13] + ν(C–C)R1 [9]
1031	1034	ν(C–C)BB [51] + ν(C–C)R1 [10] + ν(C–C)R2 [9] + ν(C–O)R3adj–O [7]
974	981	ϕ(C–C–C)R2 [28] + ν(C–C)R2 [20] + ν(C–C)R1 [10] + ν(C–C)adj–R2 [9] + ω(C=C)R2 [9] + ν(C–C)BB [8]
907	909	ϕ(C–C–C)R1 [12] + ν(C–C)R2 [12] + ν(C–C)R1 [8] + ϕ(C–C-O)adj–R3 [8] + ν(C–C)R3 [7] + ν(C–C)adj–R1 [6]
877	875	ϕ(C–C–C)R2 [28] + ν(C–C)adj–R1 [18] + ν(C–C)R2 [10] + ν(C–C)com–R1&R2 [10] + ϕ(C–C–C)R1 [7] + ν(C–C)R1 [6]
817	816	τ(C–C)R3 [18] + τ(C=C)adj–R3 [11] + ν(C–O)adj–R3 [10] + ϕ(C–C=C)BB [8] + ω(O=C)R3 [7] + ν(C–C)R3 [7] + ϕ(C–C–C)BB [6]
708	715	ϕ(C–C–C)R2 [12] + ϕ(C–C–C)adj–R1&R2 [10] + ϕ(C–C–C)R12 [10] + ν(C–O)R3adj–O [8] + τ(C–C)R3 [6] + ω(O–C)R1&R3 [5]
659	659	ϕ(C–C=C)adj–R2 [30] + ϕ(C–C–C)R2 [16] + ϕ(C–C–C) adj–R1&R2 [7] + ϕ(C–C–C)R1 [7] + ν(C–C)R1 [7]
576	572	ω(O=C)R3 [20] + ϕ(C–C–O)R3 [15] + ϕ(C–C–C)R3 [14] + ϕ(C–O–C)R3 [12] + τ(C–O)R3 [7] + τ(C–C)R3 [6]

Note: Abbreviations used in the table have following meanings: R – Ring; Adj – Adjacent to; Com – Common to; BB – Back Bone.

the experimental data has been made on the basis of potential energy distribution, line profile, relative intensities, energies and the presence/absence of a given mode in similar molecules.

Although a number of spectroscopic studies [30–33] have been performed on andrographis paniculata but presumably, the data for the normal mode analysis on andrographolide is being reported for the first time and this makes it imperative to discuss all the vibrational modes with significant potential energy distribution and hence their relation with the conformation of andrographolide (Fig. 1). All the significant vibrational modes involving the prime sites are discussed as follows:

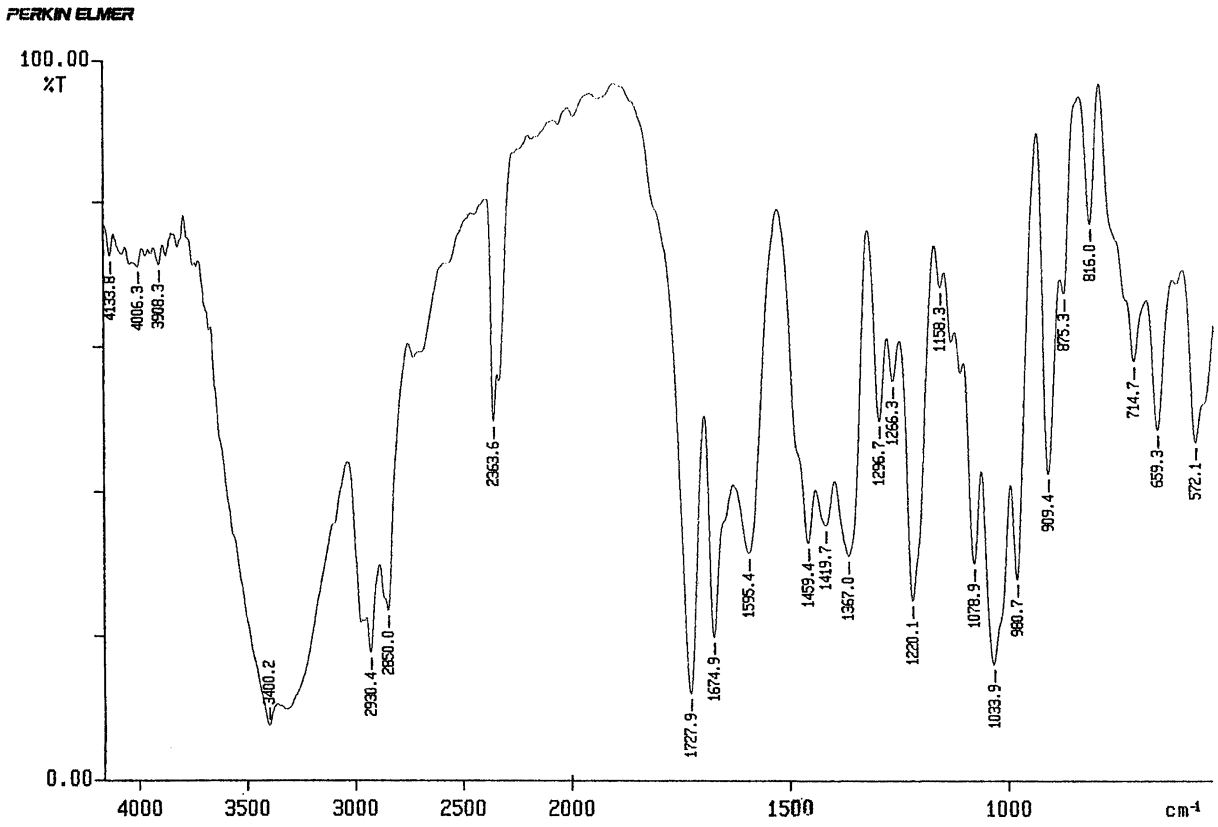

Fig. 2. FT-IR spectra of Andrographolide (4000–550) cm^{-1}.

4.3. Rings R1, R2, R3

The molecule under study is a diterpene which has C4 primary alcoholic group **(CH2–OH)** and this furan ring assumes importance because of the bioactivity point of view. As per the normal mode calculations, the stretching mode appearing at 1728 cm^{-1} has a significant potential energy distribution (P.E.D) of (C16=O23) 77%, that can be possibly explained by the fact that C16 carbonyl atom is in conjugation with C12=C13 on one end and ring O21 on the other hand. This conjugation imparts negative charge to the C=O carbon by delocalisation. The above observation can also compared with C=O stretching mode in case of gamma-butyrolactone [34] in which it appears at 1772 cm^{-1}. This value is very typical for similar modes in lactones or similar fragments [35]. The band at 572 cm^{-1} was assigned to the in-plane and out-of-plane deformations, respectively, of the carbonyl group. These assignments are based on the facts that carbonyl deformation modes do not normally give strong absorptions and occur in this general region.

As suggested by the crystallographic study and along with our normal mode calculations it can be said that the ring R3 remains in puckered form and R1, R2 in chair form, which is further, evidenced by a high percentage of potential energy distribution of (C12–C13) 47% and (C8–C17) 67%. The potential energy distribution data further suggested that C attached to the heteroatom i.e., O has high p.e.d. Value e.g. (C15–O21) 46%. The low value of (C3–O25) 22% as compared to (C14–O22) 51% is suggestive of the close proximity of C14–O22 by ring junction (C12–C11) 51% and rings R1 and R2. For the vibrational

band at 659 cm^{-1} the normal mode calculation yields a potential energy distribution with ϕ(C–C=C) 30% whereas the deformation ϕ(C–C–C) is only 16%. A lot of similarity is found between the normal mode analysis and the nmr study [30,31] performed on andrographolide. The downfield signal for H (12) was used as starting point. A decoupling experiment established couplings of 6.8 Hz to the proton at 2.63 ppm (H (11a)).

And 2.58 ppm (H (11b)). Although these protons overlap somewhat, the vicinal couplings to H (9a) (1.92 ppm) of 3.9 Hz for H (11a) and H (11b) (16.5 Hz) has been observed previously for similar systems and was attributed to the hyperconjugative effect of the vinyl group. This is also supported by the potential energy distribution of (C12–C11) 51%.

5. Conclusions

The aim of this work was to characterize the dynamics of the diterpene andrographis paniculata and based on the biochemical, spectroscopic and the present study it can be said that the plant Andrographis paniculata offers an inspiring promise in many areas of medicinal importance and requires more clinical investigation along with basic research. The normal mode analysis of andrographolide shows a dynamical behaviour and possibly, opens up an avenue for further conformational research. And lastly, receptor binding action needs to be investigated thoroughly which probably can be explained by ab initio and DFT methods and this is the subject of proposed study on andrographolide which shall be reported shortly.

The author wishes to acknowledge the support of Dr. Kanwal Raj, Medicinal and Process Chemistry Division, CDRI, Lucknow, India for the experimental and spectroscopic data on andrographolide including the sample. The author also wishes to acknowledge the help received from Prof. Sudha Jain, Chemistry Department, Lucknow University for meaningful suggestions.

References

[1] A.K. Nadkarni and K.M. Nadkarni, *Indian Materia Medica, Bombay Popular Prakashan* **1** (1976), 101–103.
[2] D. Bensky, A. Gamble and T. Kaptchuk, *Chinese Herbal Medicine Materia Medica*, Revised Ed., Seattle Eastland press, 1993, 95.
[3] K. Bone, "The Story of Andrographis paniculata, a new immune system" a herb, *Nutrition and Healing* (1998), Sept. 3,4,8,9 [review].
[4] A. Leelarasamee, A.S. Trakulsomboon and N. Sittisomoong, Undetectable antibacterial activity of andrographis paniculata (Burma) Wall.ex ness, *J. Med. Assoc. Thail.* **73** (1990), 299–304.
[5] A. Plubrukarn, S. Pinsuwan, S. Ingkatawornwong and T. Supavita, Stability of andrographolide in powdered andrographis herb under accelerated conditions, *PLANTA MEDICA* **72** (2006), 954–956.
[6] S.R. Jada, A.S. Hamzah, N.H. Lajis, M.S. Saad, M.F. Stevens and J. Stanlas, Semisynthesis and cytotoxic activities of andrographolide analogues, *J. Enzyme Inhib. Med. Chem.* **21**(2) (2006), 145–155.
[7] J.R. Hanson, Diterpenoids, *Nat. Prod. Rep.* **21** (2004), 785–793.
[8] N. Pholphana, N. Rangkadilok, S. Thongnese, S. Ruchirawat, M. Ruchirawat and J. Satyavivad, Determination and variation of three active diterpenoids in Andrographis paniculata (Burm.f) Nees, *Phytochem. Anal.* **15**(6) (2004), 365–371.
[9] L. Lomlim, N. Jirayupong and A. Plubrukarn, Heat accelerated degradation of solid-state Andrographolide, *Chem. Pharm. Bull.* **51**(1) (2003), 24–26.
[10] N. Misra, P. Tandon, V.D. Gupta and V.P. Gupta, Dynamics of Met^5 and Leu^5 enkephalin and their receptor binding activity in relation to morphine, *Indian J. Biochem. Biophys.* **31** (1994), 43–54.
[11] N. Misra, P. Tandon, V.D. Gupta, V.P. Gupta and D.C. Gupta, Recent advances in the study of neuro transmitter receptors, edited by R.S. Rapaka, *Drug Research Perspectives*, CDRI publication, **17** (1994), 403–417.
[12] N. Misra, O. Prasad, L. Sinha, G.P. Gupta, R.C. Agnihotri and J.N. Lal, Theoretical study of temperature induced phase transitions in poly(β-benzyl-L-aspartate) and its copolymer, *Polymer* **46** (2005), 7450–7455.

[13] N. Misra, O. Prasad, L. Sinha, G.P. Gupta and R.C. Agnihiotri, Pressure induced order-disorder transition in a diblock copolymer, *Polymer* **46** (2005), 11876–11880.
[14] N. Misra, O. Prasad, L. Sinha, G.P. Gupta, C. Mehrotra, R.C. Agnihotri and J.N. Lal, Theoretical study of temperature induced transition and hyper stability of collagen mimics, *Polymers* **47** (2006), 1674–1677.
[15] N. Misra, O. Prasad and L. Sinha, Vibrational dynamics of morphine in relation to Leu^5 and Met^5 enkaphalins, *Indian Journ. Biochem. Biophys.* **43** (2006), 173–181.
[16] N. Misra, O. Prasad and L. Sinha, 2006, communicated to *Biophysics (Japan)*.
[17] N. Misra, O. Prasad and L. Sinha, 2006, communicated to *Theochem.*
[18] M.T. Vijayvitthal, S. Kumar and K. Raj, Oxidation studies in Andrographolide, *Nat. Prod. Res.* (2006), Accepted (Manuscript No NPR-1–210758).
[19] E.B.Jr. Wilson, J.C. Decius and P.C. Cross, *Molecular Vibrations*, Dover Publications, New York, 1980, pp. 208–239.
[20] E.B.Jr. Wilson, A method of obtaining the expanded secular equation for the vibration frequencies of a molecule, *Chem. Phys.* **7** (1939), 1047–1052.
[21] E.B.Jr. Wilson, Some mathematical methods for the study of molecular vibrations, *J. Chem. Phys.* **9** (1941), 76–78.
[22] H.C. Urey, C.A. Bradley, The vibrations of pentatonic tetrahedral molecules, *Phys. Rev.* **38** (1931), 1969–1978.
[23] S. Gupta, M.A. Chaudhary, J.N.S. Yadav, V. Srivastava and J.S. Tandon, Anti-diarrheal activity of diterpenes of andrographis paniculata (Kal-megh) against Escheritia coli enterotoxin in in vivo models, *Int. J. Crud. Drug. Res.* (1990), 273.
[24] C. Hu, B. Zhao and Z. Caoyo, Spectrometric identification of dierpene-andrographolide, *CA* (1981), 531, 9720702m.
[25] T. Fujita, R. Fujitani, Y. Takeda, Y. Takashi, T. Yamada, M. Kido and I. Minza, X-ray studies on andrographolide, *Chem. Parm. Bull.* **32** (1984), 2117–2125.
[26] A. Basak, S. Cooper, A.G. Roberge, U.K. Banik, M. Chretiens and N.G. Seidah, Inhibition of Proprotein convertases-1,7 and furin by diterpenes of Andrographis Paniculata and their succinoyl esters, *Biochem. J.* **338** (1999), 107–113.
[27] P.L. Smith, K.N. Maloney, R.G. Pothen, J. Clardy and D.E. Clapham, Bisandro from AP activates TRPV4 Channels, *J. Biol. Chem.* **281** (2006), 29897–29904.
[28] T. Shimanouchi, *Computer Program for Normal Coordinate Treatment of Polyatomic Molecules*, University of Tokyo, 1968.
[29] A.L. Spek, A.M.J. Duisenberg and R.P. Labadie, Hydrogen bonding in Andrographolide, *Acta Cryst.* (1987), 530–532.
[30] D. Zhao, K. Liao, X. Ma and X. Yan, Study of the supramolecular Inclusion of β-Cyclodextrin with andrographolide, *J. Inclusion. Phenomenon* **43** (2002), 259–264.
[31] H.W. Xu, J. Zhang, H.M. Liu and J.F. Wang, Synthesis of andrographolide cyclophosphate derivatives and their antitumour activities, *Synthetic Communications* **36** (2006), 407–414.
[32] Y. Xinsheng, L. Xiangmin, H. Ke, Q. Feng, G. Hao, L. Jiankuan and H. Xiangjiu, Identification of a rare sulphonic acid metabolite of andrographolide in rats, *DMD* **31** (2003), 983–985.
[33] A.B. Smith, B.H. Toder, P.J. Carroll and J. Donohue, Stereochemistry of andrographolide, *J. Cryst. Spectrosc. Res.* **12**(4) (1982), 309–319.
[34] D.P. Mcdermott, Vibrational assignments and normal coordinate analyses of gamma-butyrlactone and 2-pyrrolodinones, *J. Phys. Chem.* **90** (1986), 2569–2576.
[35] R.M. Silverstein, G.C. Bassler and T.C. Morrill, *Spectrometric Identification of Organic Compounds*, 4th edn, Wiley, New York, 1981.